



ELSEVIER

Available online at www.sciencedirect.com

 ScienceDirect

Nuclear Physics A 00 (2010) 1–7



www.elsevier.com/locate/nuclphysa

Cold Nuclear Matter Effects on J/ψ Yields in d +Au Collisions at PHENIX

Matthew G. Wysocki, for the PHENIX Collaboration

Dept. of Physics, 390 UCB, University of Colorado at Boulder, Boulder, CO, 80309-0390

Abstract

The latest PHENIX measurements of J/ψ yields in d +Au collisions at $\sqrt{s_{NN}} = 200$ GeV are presented as well as the nuclear modification factor R_{dAu} and R_{CP} . The results span a wide rapidity range ($-2.2 < y < 2.4$) and are compared with several theoretical models. The data is also compared to several simple models of the geometric dependence of the nuclear modification. It is found that the forward rapidity data favor a stronger suppression than one that is linear or exponential in the density-weighted longitudinal thickness.

Keywords:

1. Introduction

J/ψ s offer a unique probe of cold nuclear matter (CNM) effects in heavy ion collisions. As gluon-gluon fusion is the dominant J/ψ production process at the Relativistic Heavy Ion Collider (RHIC), J/ψ s can offer insight into gluon shadowing and anti-shadowing, as well as gluon saturation at low x . Additionally, it is possible in heavy ion collisions to separate events by impact parameter, which offers information on the geometric dependence of the nuclear modification. Finally, it is also important to understand CNM effects on J/ψ production in order to use J/ψ s as a probe of the quark-gluon plasma.

PHENIX has recently published new results for J/ψ production in d +Au and p + p collisions at $\sqrt{s_{NN}} = 200$ GeV/nucleon using data from the 2006 and 2008 RHIC Runs [1]. The d +Au data recorded in 2008 have ~ 30 -50 times the J/ψ yield of the previous results using the 2003 d +Au dataset [2] and offer a much better constraint on the level of CNM effects. Additionally, the newer data provide better differential information through finer binning.

The PHENIX experiment measures J/ψ production through two decay channels: di-electrons at mid-rapidity and di-muons at forward and backward rapidities. The Central Arm detectors cover a rapidity range of $|y| < 0.35$, while the Muon Arm detectors cover $-2.2 < y < -1.2$ and $1.2 < y < 2.4$. Additionally, PHENIX measures the collision z position and centrality using the Beam-Beam Counters (BBCs) located at $3.0 < |\eta| < 3.9$. For an overview of the PHENIX detector systems, see [3].

The J/ψ invariant yields from $\sqrt{s_{NN}} = 200$ GeV d +Au and p + p data are shown as functions of rapidity in Figure 1. The d +Au points are scaled by $1/N_{\text{coll}}$, where N_{coll} is the average number of binary collisions, and the deviation from N_{coll} -scaling can already be seen, as well as the additional suppression at forward rapidity (the deuteron-going direction).

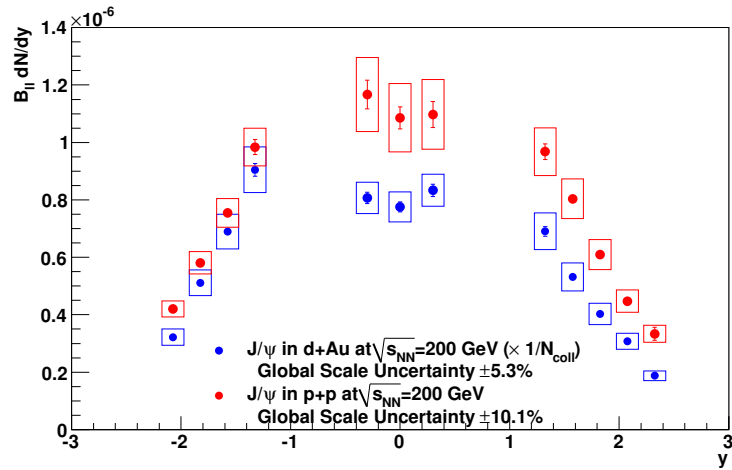


Figure 1: J/ψ invariant yields as a function of rapidity from [1]. The blue points represent the 2008 $d+Au$ data divided by N_{coll} , while the red points correspond to the combined $p+p$ datasets of 2006 and 2008. Error bars represent the statistical and uncorrelated systematic uncertainties, while the boxes represent the point-to-point correlated systematics.

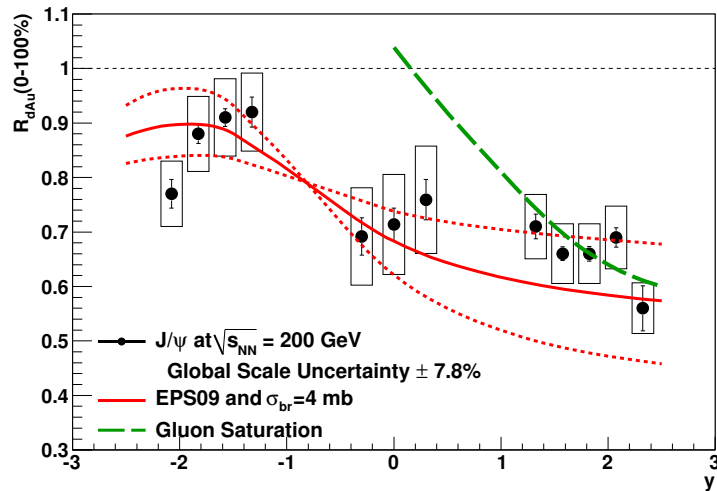


Figure 2: $J/\psi R_{dAu}$ (0-100%) as a function of rapidity. Solid red curves represent the central EPS09 nuclear-modified PDF and $\sigma_{br} = 4$ mb, while the dashed curves use the nPDFs of the set that give maximum variation. The green dashed curves is a calculation using gluon saturation at low x and enhancement from double gluon exchange [4].

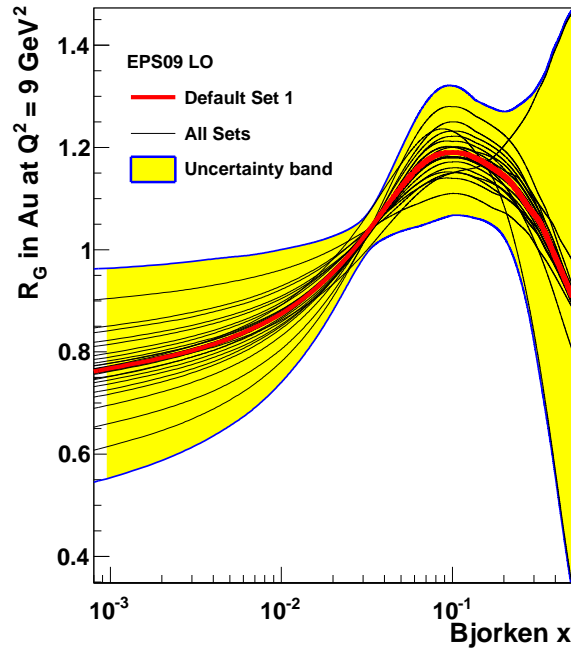


Figure 3: Nuclear modification of the gluon PDF from EPS09 [5] at $Q^2 = 9 \text{ GeV}^2$.

2. Nuclear Modification

The nuclear modification factor R_{dAu} is formed by taking the ratio of $d+Au$ to $p+p$ yields, scaled by $1/N_{\text{coll}}$:

$$R_{dAu} = \frac{1}{N_{\text{coll}}} \frac{dN_{d+Au}/dy}{dN_{p+p}/dy} \quad (1)$$

R_{dAu} for all centralities (0-100%) is shown in Figure 2. As can be seen in the Figure, there is substantial suppression at forward and mid-rapidities, as well as moderate suppression at backward rapidity. Also plotted in the figure are the predictions constructed from two different models.

The red curves use the EPS09 nuclear-modified set of parton distribution functions (PDFs) [5], as well as a break-up cross section (σ_{br}) of 4 mb for the dissociation of $c\bar{c}$ pairs in the outgoing nuclei. Because J/ψ production at RHIC is dominated by gluon-gluon fusion, the modified gluon PDF (see Figure 3) is used to calculate the modification of J/ψ production in $d+Au$ collisions. The solid red curve in Figure 2 represents the central EPS09 nPDF, while the dashed lines represent the nPDFs from the same set that give the largest variation in the rapidity regions this measurement is sensitive to. These curves have reasonable agreement with the data, with the best agreement somewhere between the default nPDF and the nPDF that gives the least suppression at forward rapidity.

The green dashed curve of Figure 2 is a calculation incorporating gluon saturation at small parton x in the gold nucleus, as well as enhancement from double gluon exchange with the nucleus [4]. As can be seen, this calculation agrees quite well at forward rapidity, but deviates quickly as the kinematics shift to mid-rapidity.

3. Geometric Dependence of Nuclear Modification

The EPS09 nPDFs do not include any geometric dependence to the PDF modification, and hence are unable to provide calculations as functions of impact parameter or centrality without additional input. Because of this, $d+Au$ measurements versus centrality offer a valuable insight into the geometric dependence of nuclear PDF modification.

Email address: wysockim@colorado.edu (Matthew G. Wysocki)

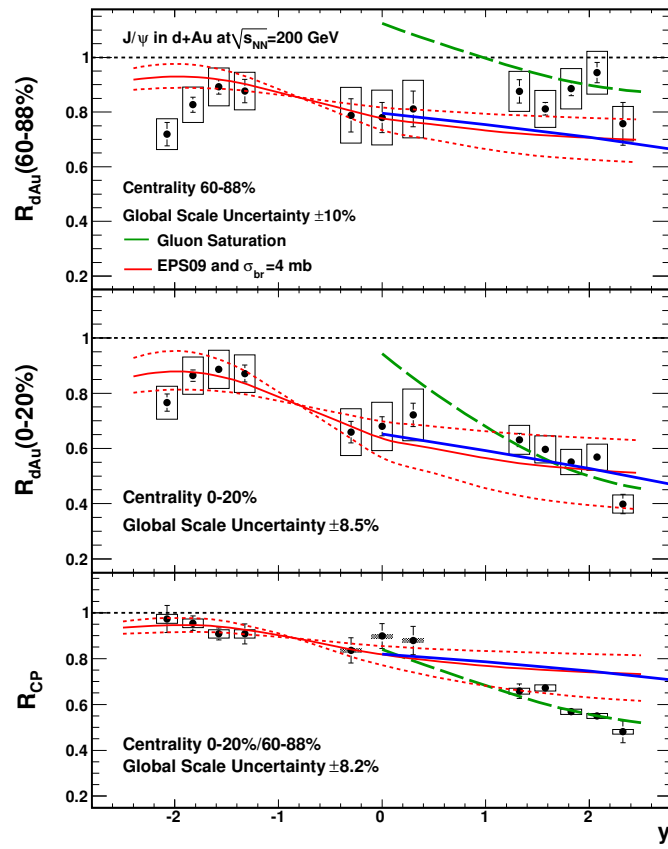


Figure 4: Top: R_{dAu} vs. rapidity for 60-88% centralities. Middle: R_{dAu} vs. rapidity for 0-20% centralities. Bottom: R_{CP} vs. rapidity using 0-20% and 60-88% centralities. All panels include the three model calculations described in the text.

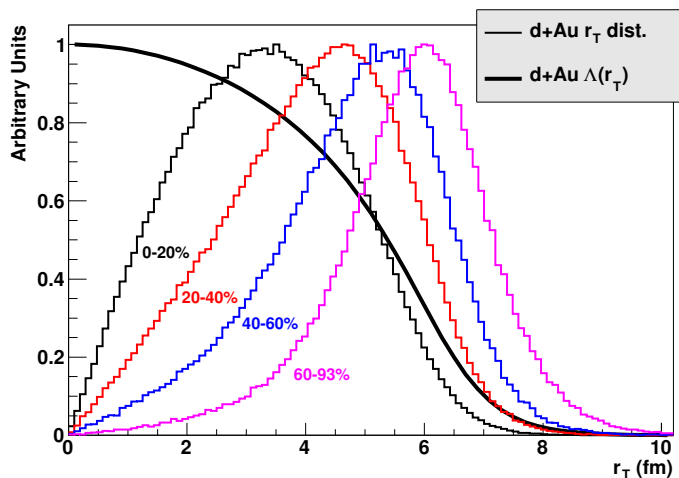


Figure 5: r_T distributions for the four centrality classes, renormalized to have the same peak height. Also shown is the integrated longitudinal density as a function of r_T using a Wood-Saxon nuclear density distribution.

The centrality of a $d+Au$ collisions is calculated by assuming that the charge deposited in the BBC in the gold-going direction monotonically increases with the mean number of participant nucleons $\langle N_{\text{part}} \rangle$ in the collision. Therefore, by dividing the BBC charge distribution into percentile bins of events, the events are divided into groups of different $\langle N_{\text{part}} \rangle$.

Finally, using a Glauber Monte Carlo [6] to throw an N_{part} event-by-event and comparing to the actual distribution from data, it is possible to calculate other average quantities for each centrality bin, such as the mean impact parameter $\langle b \rangle$ or number of binary nucleon-nucleon collisions $\langle N_{\text{coll}} \rangle$.

R_{dAu} in the most peripheral (60-88%) and most central (0-20%) bins are shown in Figure 4 versus rapidity. As can be seen, the suppression at backward rapidity is very similar between the two bins, while that at mid- and forward rapidity are more severe, particularly at forward rapidity.

In addition to R_{dAu} , the ratio can be taken between the most central and peripheral bins, $R_{CP} = R_{dAu}(0 - 20\%) / R_{dAu}(60 - 88\%)$. R_{CP} has the advantage of canceling much of the point-to-point correlated systematics of the numerator and denominator. This can be seen in the lower panel of Figure 4, and emphasizes the increase in suppression at forward rapidities (the deuteron-going direction) in central collisions.

Because the EPS09 nPDFs have no centrality dependence, this must be added retroactively with some assumption on the geometric dependence. In [7], it is assumed that there is a linear dependence on the integrated longitudinal density, and this is the calculation used for the red curves in Figure 4, based on the same EPS09 nPDF set and $\sigma_{br} = 4$ mb as the previous Figure. This gives good agreement for the most central case, but not as good for the peripheral case or R_{CP} . While σ_{br} could be reduced to improve the agreement at forward rapidity in peripheral events, this would simultaneously reduce the agreement for central collisions. In fact it is impossible for the EPS09 nPDFs and σ_{br} that is constant with rapidity to describe the data across the full range of centralities and rapidities.

Also shown in Figure 4 is the same gluon saturation calculation as shown previously, again as the green dashed lines. In this case the calculation was provided as a function of N_{coll} in several rapidity bins, which was then mapped to the PHENIX centrality classes. Again, this calculation does quite well at forward rapidity, but deviates quickly from the data as it goes to $y = 0$. For R_{CP} , however, the deviations at mid-rapidity cancel out and the curve matches the data over the calculation's rapidity range.

Using the Glauber simulation it is possible to generate the r_T distribution for each centrality class, where r_T is the transverse position of the incident nucleon in each binary $N-N$ collision. These distributions are shown in Figure 5. This is more direct than using the $d+Au$ impact parameter which, due to the size of the deuteron, can have a wide variety of $N-N$ collision positions for a given b . It is therefore preferable to fold model calculations with the r_T distribution (or equivalent) than with the $\langle b \rangle$ or $\langle N_{\text{coll}} \rangle$ distributions in order to compare to model calculations with a

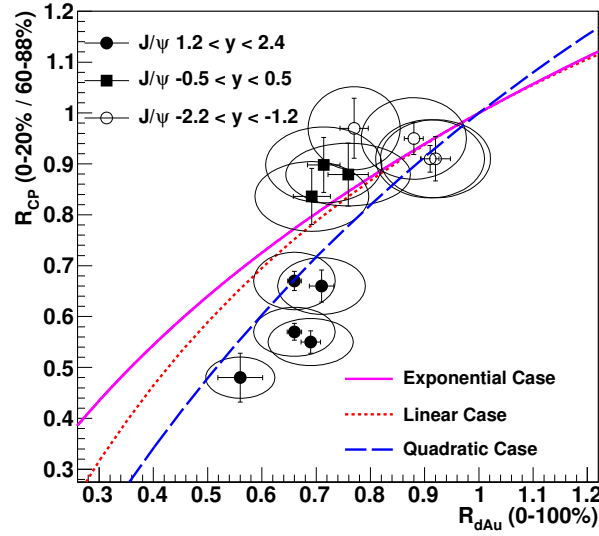


Figure 6: R_{CP} vs. $R_{dAu}(0-100\%)$ for both data and three simple models of the geometric dependence of the modification.

geometric dependence.

As an example of performing such a comparison, note that the impact parameter in $p+A$ collisions is very similar to r_T . In [8] a calculation is performed by treating the $c\bar{c}$ pre-hadronic state as coherently interacting with the nucleus, as opposed to using a break-up cross section, and the CNM suppression of J/ψ s as a function of impact parameter is calculated for $p+A$ collisions. Treating b as r_T in $d+Au$ collisions, it is trivial to fold R_{pA} with the r_T distributions for the PHENIX centrality classes and produce R_{dAu} vs. centrality. These are shown as the blue curves in Figure [?]. As can be seen, this result is very similar to the calculations using EPS09 and $\sigma_{br} = 4$ mb.

Further calculations can be performed by assuming that the position-dependent nuclear modification $M(r_T)$ is dependent on the integrated longitudinal density of the nucleus:

$$\Lambda(r_T) = \frac{1}{\rho_0} \int dz \rho(r_T, z) \quad (2)$$

as was done in [7]. In [1] several simple functional forms with a single free parameter a are used, including an exponential, linear, or quadratic dependence on Λ . To calculate R_{dAu} for any centrality bin, the modification $M(r_T)$ is folded with the r_T distribution ($f_i(r_T)$) for that bin i :

$$R_{dAu,i}(a) = \int dr_T f_i(r_T) M(r_T; a) \quad (3)$$

To extract the actual geometric dependence of the data more directly, a plot may be constructed that uses $R_{dAu}(0-100\%)$ as the x -axis to represent the overall level of modification (averaged over the entire nucleus), and $R_{CP}(0-20\%)$ as the y -axis to get the relative difference in the suppression between central and peripheral collisions. So for a fixed average modification (x -value), a steeper centrality dependence will tend to shift the y -value down (assuming the modification is a suppression).

Now the R_{dAu} and R_{CP} may be calculated using the functional forms above. As the parameter a is varied, we map out a single curve in the R_{CP} - R_{dAu} plane. This can also be thought of as a plot of the parametric equations $\{x(a), y(a)\}$. So each simple dependence on $\Lambda(r_T)$ gives us a different, single curve in the R_{CP} - R_{dAu} plane, which can be compared to the data. This is plotted Figure 6. As would be expected, all cases converge to (1,1) when the parameter a goes to zero.

The data points each represent a rapidity bin, and the ellipses represent the one-standard-deviation contours of the point-to-point correlated and global systematic uncertainties, which are mostly uncorrelated between R_{CP} and

$R_{dAu}(0-100\%)$. As can be seen, the backward and mid-rapidity data are unable to separate the difference cases, but the forward rapidity data favors a dependence on $\Lambda(r_T)$ stronger than either linear, exponential, or quadratic.

It should be noted that should multiple effects be combined with more than one free parameter, the curves need not necessarily converge at (1,1). For example, in such a situation it is possible to have no modification on average ($R_{dAu}=1$), but have an enhancement in peripheral collisions that cancels with suppression in central collisions when averaging, but leads to $R_{CP} \neq 1$.

4. Conclusion

The latest PHENIX $d+Au$ data has been presented and compared to several model calculations for cold nuclear matter effects. As has been noted, folding model calculations with the r_T distribution for a given centrality class is a more accurate way to map to the PHENIX centrality definitions than by folding with some already-averaged quantity such as $\langle N_{coll} \rangle$.

Additionally, the geometric dependence of the nuclear modification was directly explored by combining both $R_{dAu}(0-100\%)$ and R_{CP} measurements. Comparing these to simple functional forms for the geometric dependence, it was found that the forward rapidity data require a stronger suppression than one which is linear or exponential with the density-weighted nuclear thickness.

One possible CNM effect that is not explored here is initial-state parton energy loss, *i.e.* energy loss of the incoming gluon passing through the gold nucleus before the hard scattering. It is possible that such an effect could enhance the suppression seen at forward rapidity in the data. Previously this has been studied with Drell-Yan measurements at lower CMS energies, see *e.g.* [9, 10, 11]. For several calculations involving this effect for J/ψ production in $d+Au$ collisions, see [12].

MGW acknowledges funding from the Division of Nuclear Physics of the U.S. Department of Energy under Grant No. DE-FG02-00ER41152.

References

- [1] A. Adare, et al., Cold Nuclear Matter Effects on J/ψ Yields as a Function of Rapidity and Nuclear Geometry in Deuteron-Gold Collisions at $\sqrt{s_{NN}} = 200$ GeV [arXiv:1010.1246](#).
- [2] A. Adare, et al., Cold nuclear matter effects on j/ψ production as constrained by deuteron-gold measurements at $\sqrt{s_{NN}} = 200$ gev, *Phys. Rev. C* 77 (2) (2008) 024912. [arXiv:0711.3917](#), doi:10.1103/PhysRevC.77.024912. URL <http://link.aps.org/abstract/PRC/v77/e024912>
- [3] K. Adcox, et al., Phenix detector overview, *Nucl. Inst. and Meth. A* 499 (2-3) (2003) 469–479. doi:10.1016/S0168-9002(02)01950-2. URL [http://dx.doi.org/10.1016/S0168-9002\(02\)01950-2](http://dx.doi.org/10.1016/S0168-9002(02)01950-2)
- [4] D. Kharzeev, K. Tuchin, Signatures of the color glass condensate in J/ψ production off nuclear targets, *Nucl. Phys. A* 770 (2006) 40–56. doi:10.1016/j.nuclphysa.2006.01.017.
- [5] K. J. Eskola, H. Paukkunen, C. A. Salgado, EPS09 - a New Generation of NLO and LO Nuclear Parton Distribution Functions, *JHEP* 04 (2009) 065. doi:10.1088/1126-6708/2009/04/065.
- [6] M. L. Miller, K. Reygers, S. J. Sanders, P. Steinberg, Glauber modeling in high energy nuclear collisions, *Annu. Rev. Nucl. Part. Sci.* 57 (2007) 205–243. [arXiv:nucl-ex/0701025](#), doi:10.1146/annurev.nucl.57.090506.123020. URL <http://arxiv.org/abs/nucl-ex/0701025>
- [7] S. R. Klein, R. Vogt, Inhomogeneous Shadowing Effects on J/ψ Production in dA Collisions, *Phys. Rev. Lett.* 91 (2003) 142301. [arXiv:nucl-th/0305046](#), doi:10.1103/PhysRevLett.91.142301.
- [8] B. Z. Kopeliovich, I. K. Potashnikova, H. J. Pirner, I. Schmidt, Heavy quarkonium production: Nontrivial transition from pA to AA collisions [arXiv:1008.4272](#).
- [9] J. Moss, G. Garvey, M. Johnson, M. Leitch, P. McGaughey, et al., Energy loss of fast quarks in nuclei (2001) 576–580 [arXiv:hep-ex/0109014](#).
- [10] M. B. Johnson, et al., Energy loss versus shadowing in the Drell-Yan reaction on nuclei, *Phys. Rev. C* 65 (2002) 025203. doi:10.1103/PhysRevC.65.025203.
- [11] R. Neufeld, I. Vitev, B. Zhang, Toward a determination of the shortest radiation length in nature [arXiv:1010.3708](#).
- [12] J. Nagle, A. Frawley, L. L. Levy, M. Wysocki, Theoretical Modeling of J/ψ Yield Modifications in Proton (Deuteron) - Nucleus Collisions at High Energies [arXiv:1011.4534](#).